Unbound and Acylated Structures of the MecR1 Extracellular Antibiotic-sensor Domain Provide Insights into the Signal-transduction System that Triggers Methicillin Resistance

ARTICLE *in* JOURNAL OF MOLECULAR BIOLOGY · SEPTEMBER 2006

Impact Factor: 4.33 · DOI: 10.1016/j.jmb.2006.06.046 · Source: PubMed

5 AUTHORS, INCLUDING:

Tibisay Guevara
Molecular Biology Institute of Barcelona
22 PUBLICATIONS **241** CITATIONS
SEE PROFILE

Raquel Garcia-Castellanos
IRB Barcelona Institute for Research in Biomedicine
17 PUBLICATIONS **301** CITATIONS
SEE PROFILE

Volume 361, Number 3, 18 August 2006

ISSN 0022-2836

ELSEVIER

JMB

JOURNAL OF MOLECULAR BIOLOGY

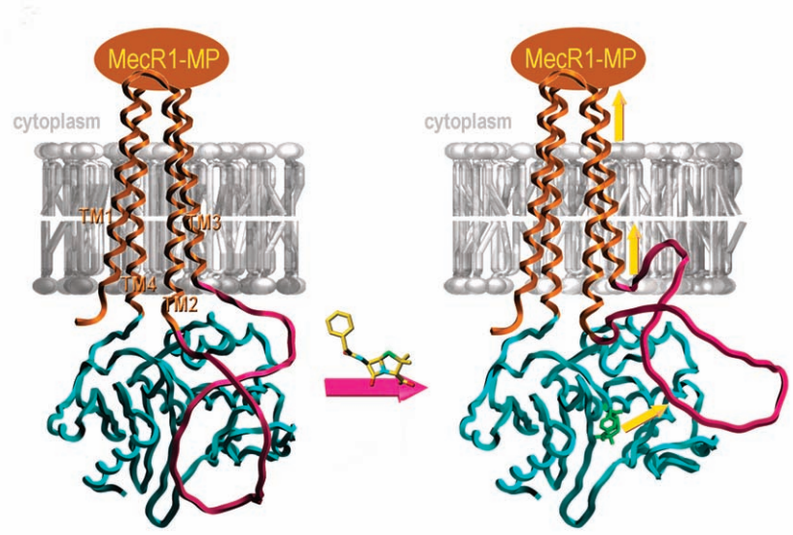

0022-2836(20060818)361:3;1-F

doi:10.1016/j.jmb.2006.06.046 J. Mol. Biol. (2006) 361, 506–521

JMB

Available online at www.sciencedirect.com

SCIENCE DIRECT®

ELSEVIER

Unbound and Acylated Structures of the MecR1 Extracellular Antibiotic-sensor Domain Provide Insights into the Signal-transduction System that Triggers Methicillin Resistance

Aniebrys Marrero, Goretti Mallorquí-Fernández, Tibisay Guevara Raquel García-Castellanos and F. Xavier Gomis-Rüth*

Institut de Biologia Molecular de Barcelona, C.I.D.–C.S.I.C. C/Jordi Girona, 18–26 08034 Barcelona, Spain

Methicillin-resistant *Staphylococcus aureus* (MRSA) strains are responsible for most hospital-onset bacterial infections. Lately, they have become a major threat to the community through infections of skin, soft tissue and respiratory tract, and subsequent septicaemia or septic shock. MRSA strains are resistant to most β-lactam antibiotics (BLAs) as a result of the biosynthesis of a penicillin-binding protein with low affinity for BLAs, called PBP2a, PBP2′ or MecA. This response is regulated by the chromosomal *mec*-divergon, which encodes a signal-transduction system including a transcriptional repressor, MecI, and a sensor/transducer, MecR1, as well as the structural *mecA* gene. This system is similar to those encoded by *bla* divergons in *S. aureus* and *Bacillus licheniformis*. MecR1 comprises an integral-membrane latent metalloprotease domain facing the cytosol and an extracellular sensor domain. The latter binds BLAs and transmits a signal through the membrane that eventually triggers activation of the metalloprotease moiety, which in turn switches off MecI-induced repression of *mecA* transcription. The MecR1 sensor domain, MecR1-PBD, reveals a two-domain structure of α/β-type fold reminiscent of penicillin-binding proteins and β-lactamases, and a catalytic serine residue as the ultimate cause for BLA-binding. Covalent complexes with benzylpenicillin and oxacillin provide evidence that serine acylation does not entail significant structural changes, thus supporting the hypothesis that additional extracellular segments of MecR1 are involved in signal transmission. The chemical nature of the residues shaping the active-site cleft favours stabilisation of the acyl enzyme complexes in MecR1-PBD, in contrast to the closely related OXA β-lactamases, where the cleft is more likely to promote subsequent hydrolysis. The present structural data provide insights into the *mec*-encoded BLA-response mechanism and an explanation for kinetic differences in signal transmission with the related *bla*-encoded systems.

Keywords: bacterial antibiotic resistance; MecR1 protein; methicillin resistance; penicillin-binding protein; MRSA; β-lactamase

*Corresponding author

Introduction

The capacity of pathogenic bacteria to develop resistance to antibiotics has led to both the need for new therapeutic approaches and the quest for a deeper understanding of the mechanisms involved. *Staphylococcus aureus* easily acquires and develops tools for resistance against antimicrobials and, in particular, its methicillin-resistant variant (MRSA) causes serious health problems through nosocomial

Abbreviations used: MRSA, methicillin-resistant variant of *Staphylococcus aureus*; PG, peptidoglycan; NAG, *N*-acetylglucosamine; NAM, *N*-acetylmuramic acid; PBP, penicillin-binding protein; BLA, β-lactam antibiotic; AEC, acyl enzyme complex; TM, transmembrane.

E-mail address of the corresponding author: xgrcri@ibmb.csic.es

and community-onset bacterial infections.[1–4] A characteristic feature of bacteria is the cell wall, required to withstand osmotic pressure and to maintain the characteristic cell morphology. The cell wall is composed mainly of peptidoglycan (PG) and other polysaccharides, whose homeostasis comprises a balance between biosynthesis and degradation.[5–7] The basic structure of a PG is a linear glycan backbone composed of alternating *N*-acetylglucosamine (NAG) and *N*-acetylmuramic acid (NAM; the ether of D-lactic acid and NAG) sugar moieties linked by β-1,4 glycosidic bonds (Figure 1(a)).[8] These glycan backbones are cross-linked by peptide bridges to create a three-dimensional meshwork sacculus with a porous surface probably with a distorted honeycomb pattern.[9–11] This leads to a typical cell-wall thickness of 20–40 nm and the rigidity needed to enclose and protect the cell. Cross-links are mediated by so-called stem peptides of sequence L-Ala-γD-Glu-L-Lys-D-Ala-D-Ala that are attached in *S. aureus* to the NAM units *via* their D-lactyl moieties before becoming connected to NAG monosaccharides. These stem peptides are connected with pentaglycine bridges that are created by the subsequent attachment of up to five glycine units (three glycine plus two L-Ser residues have been reported)[12] to the N^{η} atom of stem peptide lysine residues. These sequential reactions are carried out in *S. aureus* by the peptidyl transferases FemA, FemB and FemX.[13,14] Thereupon, a stem-peptide-bound pentaglycine is linked to the penultimate alanine residue of another stem peptide during a transpeptidase reaction (Figure 1(a)), which constitutes the terminal step in bacterial cell-wall synthesis.[15] Transpeptidation implies the removal of the fifth stem-peptide alanine residue and is catalysed by penicillin-binding proteins (PBPs)[16–18] which can further exert transglycosylase and (carboxy)peptidase activities as part of PG homeostasis. PBPs are present in all eubacteria and either four[12,19] or five[20] have been reported for *S. aureus*.

β-Lactam antibiotics (BLAs), like the classical penicillins, cephalosporins, cephamycins and cephabacins; and the novel non-conventional clavams, carbapenems, monobactams and nocardicins, interfere with PG homeostasis, targeting PBPs.[21–23] BLA activity is attributable to the structural similarity of the chemical warhead of BLAs, a central four-membered lactam ring, with the peptide bond linking the two terminal dextro alanine residues of stem peptides, which are bound and split by PBPs. (Figure 1(a) and (b)).[24,25] Due to the absence of PG and PBPs from higher organisms, BLAs are among the most popular antimicrobials in human and animal health care. However, bacteria have become able to evade their action by development of β-lactamases, alias penicillinases, which are hydrolytic enzymes that transform the lactams into the corresponding innocuous acids. PBPs and β-lactamases are related sequentially and architecturally and can be found either soluble or anchored to the bacterial cytoplasmic membrane facing the extracellular space. They are subdivided into low molecular weight (LMW) and high molecular weight (HMW) forms and are predominantly serine transferases showing similarities to serine proteases like trypsins and subtilisins in an interesting case of convergent evolution.[18,26,27] In both enzyme classes, active-site serine residues are responsible for the cleavage of amide bonds through the nucleophilic attack of the serine O^{γ} atom onto the amide carbonyl group of a substrate scissile bond with participation of a general base that abstracts the proton attached to the serine oxygen atom, although it must be mentioned that the mechanistic steps leading to acylation and deacylation are different in either enzyme class. The nucleophilic attack results in a negatively charged tetrahedral intermediate that is resolved into a covalent acyl enzyme complex (AEC). The subsequent step comprises the hydrolysis of the AEC ester bond in proteases and β-lactamases. In PBPs, formation of the AEC is followed by a transpeptidation that entails the attack of the α-amino group of a pentaglycine bridge of a vicinal stem peptide onto the AEC (Figure 1(a) and (b)).[18,19,27,28] As BLAs mimic the terminal part of a pentaglycine, they can lead to AECs with PBPs which, in contrast to β-lactamases, break down very slowly, following a time-scale in the range of a complete bacterial growth-cycle. An explanation for this sluggish hydrolysis of the PBP/BLA AEC could be that the physiological transpeptidase reaction does not comprise such a solvent-mediated hydrolysis step, so that the enzyme is not prepared for it (Figure 1(a)). The stability of the PBP/BLA AEC results in a *de facto* blocked enzyme that is no longer capable of participating in bacterial cell-wall cross-linking. Although this does not lead to a fragile cell wall or direct bacteriolysis, it affects septum formation during binary fission and this eventually triggers cell death.[6]

MRSA and pre-MRSA strains like N315 produce another PBP, termed MecA, alias PBP2a and PBP2′, which is much less sensitive to BLAs.[29] MecA is a membrane-bound 78-kDa HMW class-B PBP that mediates resistance to methicillin and to the entire class of β-lactam compounds.[30–32] It acts as a surrogate enzyme when the housekeeping BLA-sensitive PBP complement has been inactivated,[33,34] and assumes the cell-wall transpeptidase function in collaboration with the transglycosylase domain of the intrinsic PBP2.[34] MecA is encoded by *mecA*, localised within DNA regions called *mec* or staphylococcal chromosome cassettes *mec*.[30,35,36] MecA-synthesis is regulated by a signal-transduction system consisting of a sensor/signal transducer, MecR1, and a transcriptional repressor, methicillin repressor MecI, both coded for by *mec* in tandem immediately upstream of the *mecA* promoter and counter-transcribed.[1,37–39] MecI regulates the whole divergon and, therefore, its own biosynthesis and that of MecA and MecR1. The MecR1-MecI-MecA axis is homologous to that encoded by the *S. aureus bla* divergon, BlaR1-BlaI-BlaZ (alias BlaR-BlaI-BlaP and PenJ-PenI-PenP) and to another one encoded by *Bacillus licheniformis* (BlaR-BlaI-BlaP). These two axes

lead to biosynthesis of the BlaZ/BlaP/PenP β-lactamases.[37,40–42]

MecI is a 123 amino acid residue protein with an N-terminal winged-helix DNA-binding domain and a C-terminal triple-helical dimerisation domain forming a spiral staircase.[43,44] MecI shares a significant degree of sequence similarity with *S. aureus* BlaI and *B. licheniformis* BlaI/PenI, and the *S. aureus*

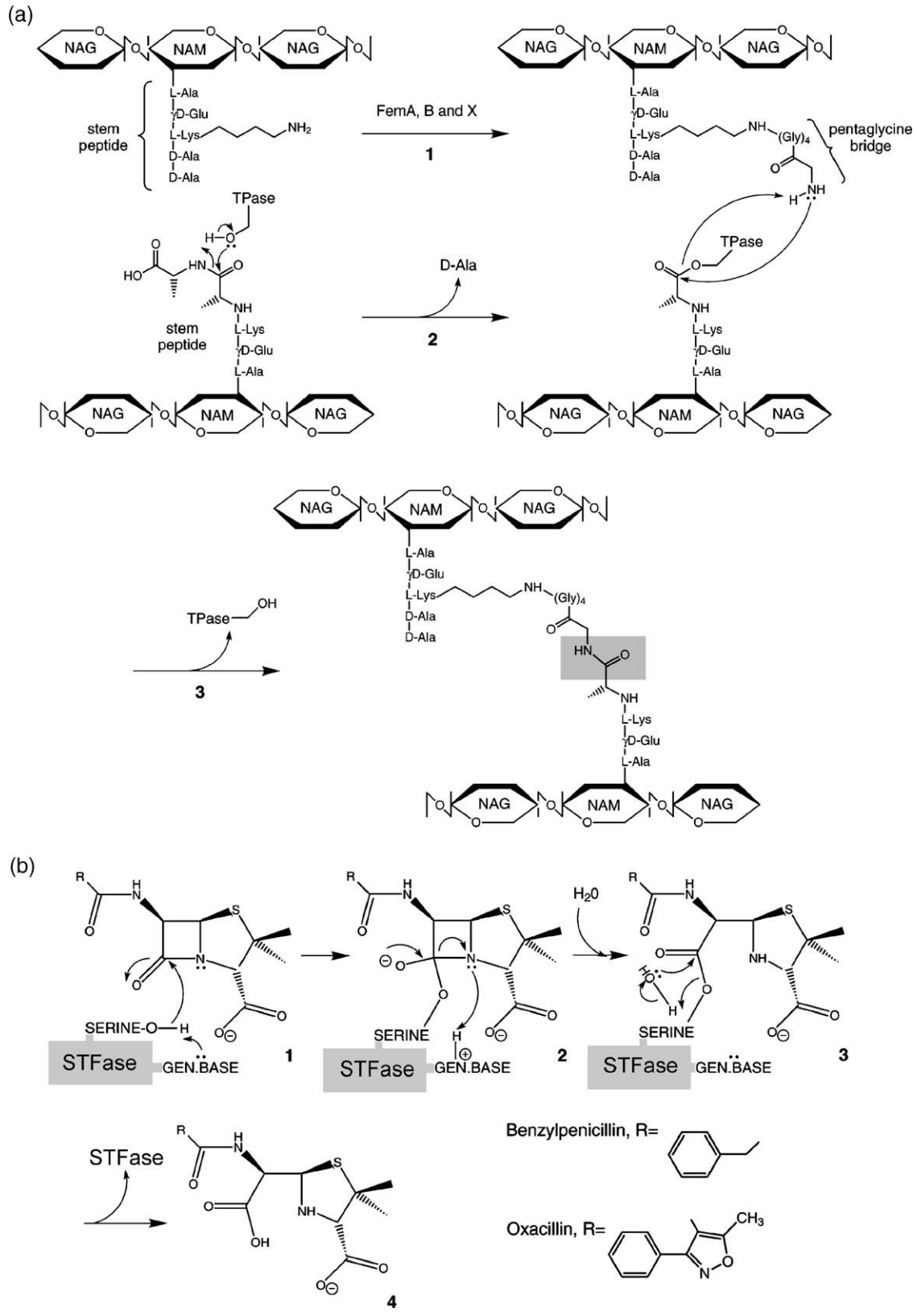

Figure 1 (*legend on opposite page*)

repressors seem to be interchangeable to block transcription of both structural and regulatory genes.[45] Highly similar sequences are found in a number of bacterial genomes.[43] MecR1 in turn is an HMW class-C PBP similar to *S. aureus* BlaR1 and *B. licheniformis* BlaR.[18,46] A more recent classification ascribes these proteins to group II of Ser-Xaa-Xaa-Lys acetyl transferases (Xaa for any amino acid).[12] Proven and potential orthologues are present in *Staphylococcus sciuri*, *Staphylococcus epidermis* and *Staphylococcus haemolyticus*, as well as in a series of bacterial genomes.[44] MecR1 is composed of an N-terminal cytosolic transmembrane (TM) zinc-dependent metalloprotease moiety (MecR1-MP) and a C-terminal extracellular domain reminiscent of single-domain PBPs (MecR1-PBD). The latter acts as a sensor for environmental BLAs and shows notable sequence similarity to LMW class-D β-lactamases.[18,42] On the basis of biochemical data, mainly from the homologous *bla* divergon proteins, the MecR1/MecI system is thought to work as follows.[44,47,48] In the basal state, MecI constitutively blocks transcription of *mecA* and *mecR1-mecI* genes as a dimer, while the MecR1-MP domain is zymogenic. If MecR1 detects BLAs in the extracellular space *via* MecR1-PBD, it becomes acylated at its active-site serine residue. This triggers the (auto)catalytic activation of the MP domain, which faces the cytosol. The active protease induces proteolytic inactivation of MecI allowing the structural *mecA* gene to be transcribed, exerting the resistance response.

We have recently solved the structure of methicillin inhibitor, MecI, isolated and in complex with cognate DNA.[43,44,48] To continue our studies on the molecular determinants of methicillin resistance in *S. aureus*, we have synthesised and purified the extracellular domain of MecR1 and analysed its 3D structure, both unbound and in covalent complexes with benzylpenicillin and oxacillin. The structure of MecR1-PBD complements previous studies on the equivalent domains of *S. aureus* BlaR1,[49,50] and *B. licheniformis* BlaR.[51] It enables us to propose a new mechanism for the activation of these sensor/signal transducers and provides new insights into the working model of the response of MRSA to antibiotic stress.

Results and Discussion

Structure analysis of unbound and acylated MecR1-PBD

MecR1-PBD was produced by recombinant over-expression in *Escherichia coli* as a construct that encoded the protein sequence from Ser334 to Ile585, plus three extra residues, Gly331, His332 and Met333 (see Materials and Methods). The 3D structures of the unbound protein and of its complexes with benzylpenicillin and oxacillin, obtained in two different space groups, were solved applying Patterson search techniques and were defined from Asp340, Gly331 and Asp340, respectively, to Ile585. In the benzylpenicillin complex, the complete N-terminal segment is clearly defined by electron density and is helical until Gln338, thus mimicking the final part of a (predicted) TM helix preceding the MecR1-PBD domain (Figure 2; and see below). This entails that this domain starts at Gln339 in MecR1. Furthermore, both BLAs are observed unambiguously in the benzylpenicillin and oxacillin complexes as covalent adducts of the catalytic serine residue, thus featuring the AECs (Figure 3(a)–(c)). The BLA atoms have been refined at full occupancy, rendering no positive or negative ($mF_{obs}-DF_{calc}$)-type electron density, as well as average *B*-factors (41.5 Å^2 for the BLA atoms in the benzylpenicillin complex and 51.9 Å^2 for those in the oxacillin complex) that are similar to those of the protein atoms in either structure (see Table 1).

The unbound MecR1-PBD structure showed a clear extra electron density close to the side-chain of His450. After several trials, it was interpreted tentatively as an ion, co-ordinated by His450 N$^{\varepsilon 2}$ (2.1 Å) and by a peptide of putative sequence glycine-histidine-methionine-serine (termed Gly1B-Ser4B) which would correspond to the N terminus

Figure 1. Serine transferase reactions. (a) PG cross-linking reactions in *S. aureus*.[7,19,88] Stem peptides are attached to the NAM modules of the glycan backbone through the D-lactyl moieties of the latter. The amidic linkage between the D-Glu and the L-Lys residue is through the γ-carboxylate group of the former instead of the α-carboxylate group. Stem peptides participate in two reactions, the attachment of a pentaglycine-bridge to the ε-amino group of the L-Lys residue, catalysed by FemA, B and X (1); and the first step of the transpeptidase reaction (2) catalysed by a PBP acting as a transpeptidase (TPase). This step entails removal of the C-terminal D-Ala and the acylation of the PBP active-site serine residue. Subsequently, the second step of the transpeptidase reaction consists of the attack of the N terminus of another pentaglycine on the ester (3), resulting in a novel isopeptidic PG cross-link (shaded frame) and regeneration of the TPase. (b) Serine transferase reaction with BLAs. The catalytic serine O$^{\gamma}$ atom of the serine transferase (STFase), which can be either a PBP TPase, a PBD or a β-lactamase, performs a nucleophilic acid substitution on the β-lactam carbonyl group under proton abstraction by a general base (1).[19] This reaction results in a negatively charged tetrahedral intermediate (2) that evolves to the AEC (3). This is the *de facto* endpoint state of the reaction of BLAs with PBP TPases and PBDs. β-Lactamases are capable of carrying out the final hydrolysis to the respective penicilloic acid in the case of penicillinase-sensitive BLAs (4), in this manner inactivating them and regenerating the STFase. This step comprises attack of a solvent molecule, directly or *via* a (second) general base, onto the acyl ester carbonyl group. The BLAs assayed in this study are (2S, 5R, 6R)-6-(benzoylamino)-3,3-dimethyl-7-oxo-4-thia-1-azabiciclo[3.2.0]heptane-2-carboxylic acid alias penicillin G and benzylpenicillin and the β-lactamase resistant but OXA-sensible (2S, 5R, 6R)-6-([(5-methyl-3-phenyl-4-isoxazolyl) carbonyl]amino)-3,3-dimethyl-7-oxo-4-thia-1-azabiciclo[3.2.0]heptane-2-carboxylic acid alias oxacillin and prostaphlin. The hydrolysis of the β-lactam to the corresponding penicilloic acid occurs under maintenance of the configuration of the three chiral centres.

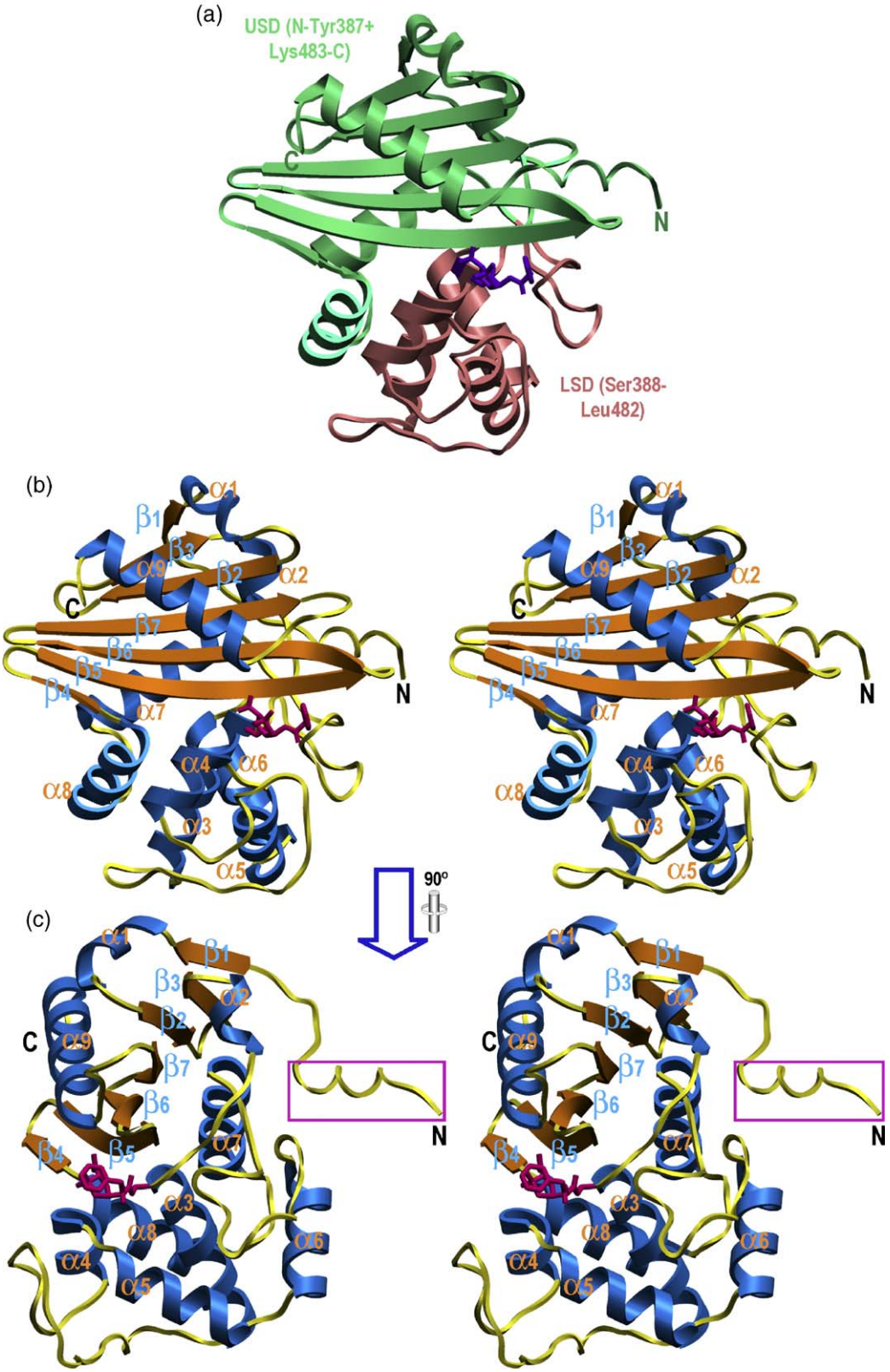

Figure 2. MecR1-PBD structure. (a) MecR1-PBD shown in the standard orientation characteristic for proteases with the two subdomains, USD and LSD, distinctly coloured. The bound benzylpenicllin moiety is shown as violet sticks. (b) Stereo-drawing showing the Richardson-diagram[89] of MecR1, orientation as in (a). β-Strands (β1-β7), as orange arrows, and helical segments (α1-α9), as blue ribbons, are shown and labelled, as are the N terminus and the C terminus. The bound benzylpenicillin moiety, as magenta sticks, pinpoints the active-site cleft. (c) Same as (b) after a vertical clockwise rotation of 90°. The protruding N-terminal segment of the crystallised construct (magenta frame) adopts a helical conformation, thus mimicking the preceding transmembrane helix in the full-length protein.

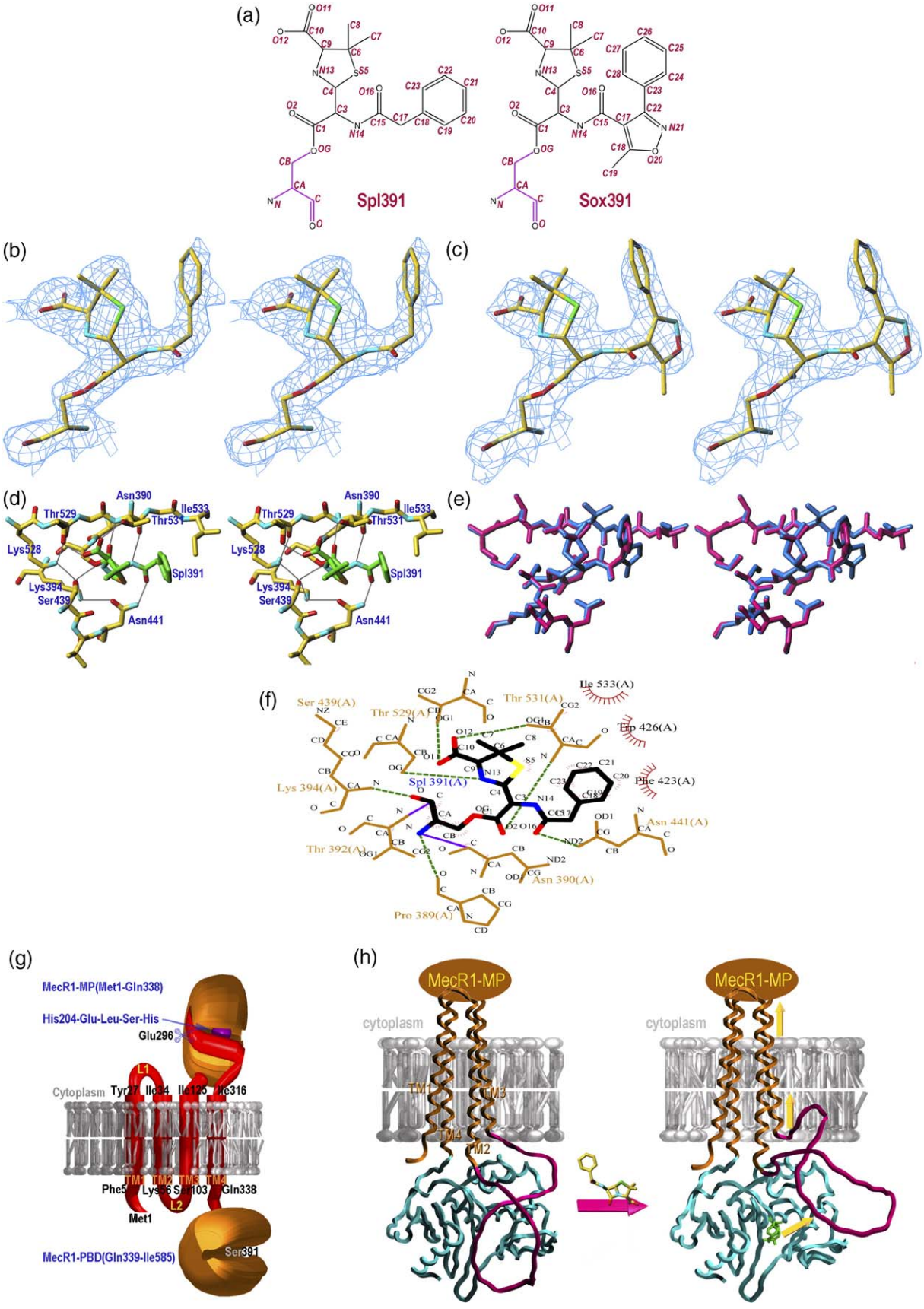

Figure 3 (*legend on next page*)

of the crystallised protein as a result of proteolytic cleavage during purification. Ion binding is exerted *via* atoms Gly1B N (2.6 Å), His2B N (2.1 Å) and His2B Nδ1 (2.1 Å), all roughly in a plane with His450 $N^{\varepsilon 2}$ and the ion. A solvent molecule, Wat615W (2.4 Å), would complete a square pyramidal coordination. This geometry, together with the nature of and the distances to the suggested ligands,[52,53] and a refined *B*-factor similar to that of surrounding atoms, suggested the ion was nickel(II). However, as this feature was not encountered in any of the acylated structures, its significance remains unclear and a purification artefact cannot be excluded.

Overall structure of MecR1-PBD

MecR1-PBD is ellipsoidal, with maximal dimensions of ~49 Å×48 Å×41 Å. The analogy with trypsin-like serine proteases can be extended to the architecture, and the protein can be displayed according to the standard orientation of the latter,[54] i.e. looking frontally onto the molecule with the active-site cleft traversing the molecular surface horizontally. This view enables us to divide MecR1-PBD into an upper subdomain (USD) and an inserted lower subdomain (LSD) (Figure 2(a)). The USD runs from the N terminus on the back surface to Tyr387, and from Lys483 to the C-terminal Ile585. It is characterised by an α-β-α sandwich topology pivoting around a central seven-stranded β-sheet, an architecture that is reminiscent of the N-terminal or upper domain of certain MPs, like *Bacillus thermoproteolyticus* thermolysin and members of the metzincin clan of MPs.[27,55,56] The sheet spans the entire upper subdomain width of MecR1-PBD and is composed of three parallel/antiparallel strands (β1–β3) provided by the part of the USD preceding the LSD insertion, and by four antiparallel strands, which are linked by simple up-and-down connectivity, downstream of the LSD. The sheet shows a +2,−1,+5×,−1,−1,−1 strand connectivity[57] and is rotated ~15° clockwise about a horizontal axis (Figure 2(c)). The sheet acquires a clockwise twist of ~75° from the short first strand β1 in the upper back of the molecule to the outermost strand β4 in the lower front, creating a concave side above and a convex side below the sheet (Figure 2(b)). The concave surface is paved with hydrophobic side-chains that mediate the interaction with two helices, α9 and 3_{10}-helix α1, which fit snugly into the concave depression. The helices run antiparallel to each other and interact through apolar contacts. Similarly, mainly hydrophobic interactions glue helices α2, α7 and α8 to the lower convex sheet surface. The LSD encompasses residues Ser388 to Leu482 and is a four-helix bundle composed of α3, α4, α5 and α6 (Figure 2(b) and (c)). The subdomain is held together by mostly aliphatic and a few aromatic contacts mediated by helical side-chains facing the inner subdomain core. Two long insertions, the loop segments between helix α3 and α4 (Lα3α4), and between α6 and α7 (Lα6α7 alias Ω-loop, reminiscent of β-lactamases)[28] are of structural importance, as they contribute to the active-site cleft (see below). Lα3α4 creates a flap on the subdomain front and is folded back to cover the LSD. It has a hairpin-like structure with the extended segments Glu413–Gln415 and Asp429–Asn431 running in an antiparallel manner and the embedded residues opening up in a wide loop (Figure 2(b)). Lα6α7 shapes the right outermost part of the subdomain and is anchored to it mainly through hydrophobic interactions with helices α5 and α6.

Figure 3. The MecR1-PBD-bound β-lactam antibiotics and working model hypothesis for MecR1-mediated signal transduction. (a) Scheme of the atom numbering of the acylated serine residues in the MecR1-PBD/oxacillin complex (modified residue Sox391; right) and in the MecR1-PBD/benzylpenicillin complex (modified residue Spl391; left) adopted in the present study. (b) Stereo-cartoon with a detail of the initial σ_A-weighted ($2mF_{obs}–DF_{calc}$)–type omit electron density map contoured at 0.8 σ above background superimposed with the final refined model centred on the benzylpenicilloyl-acylated serine (Spl391). The model employed for phasing comprised an unmodified serine at this position. (c) Same as in (b) but referred to the MecR1–PBD/oxacillin complex and the oxacilloyl-acylated serine Sox391. (d) Detail of the final refined model centred on the active site of the MecR1–PBD/benzylpenicillin complex in stereo. Protein residues contained in the three characteristic active-site motifs (see also Figure 4) and responsible for BLA-binding/stabilisation of the tetrahedral intermediate and the final adduct are shown as sticks in atom-colour mode (with carbon atoms in yellow). The carbon atoms of the penicilloyl moiety are displayed in green for clarity. Hydrogen bonds are disclosed as grey lines. The same interactions were observed in the MecR1–PBD/oxacillin complex. (e) Superimposition of the region presented in (d) of both MecR1–PBD/BLA complexes, the benzylpenicilloyl complex in magenta and the oxacilloyl complex in blue. (f) A drawing of the active-site interactions in the benzylpenicilloyl AEC. Residue Spl391 is shown as sticks emulating the atomic bonds and coloured according to the atoms connected (carbon atoms in black, oxygen atoms in red, nitrogen atoms in blue and the sulphur atom in yellow). Further protein residues are displayed as brown sticks and labelled. Residues and atoms engaged in hydrophobic interactions are characterised by red-dashed auras. (g) A representation of the postulated topology of MecR1. The (pro)metalloprotease domain (MecR1-MP) comprises residues Met1 to Gln338 and includes four TM helices, TM1 to TM4. The extracellular sensor domain (MecR1-PBD) runs from Gln339 to Ile585. The predicted extension of each of the TM-helices, the loops connecting TM1 with TM2 (L1) and TM2 with TM3 (L2), the predicted MP-domain activation cleavage point (after Glu296)[47] the MecR1-PBD active-site serine residue Ser391, as well as the metalloprotease zinc-binding consensus sequence His204–His208,[47] are indicated. (h) Scheme depicting the proposed working mechanism of MecR1 and related BlaR1/BlaR proteins upon β-lactam acylation. Modelled TM regions and loop L1 are in orange, loop L2 is in magenta and the MecR1-PBD domain is in blue. The bound benzylpenicillin in the right panel is in green. Yellow arrows pinpoint the rearrangements suggested to occur upon BLA binding, which result in the activation of the intracellular metalloprotease domain.

Table 1. Crystallographic statistics

Dataset	MecR1-PBD	MecR1-PBD/Penicillin G	MecR1-PBD/Oxacillin
Beamline/detector	ESRF BM16/MarCCD 165 mm	ESRF ID14eh2/ADSC Quantum4	ESRF ID14eh2/ADSC Quantum4
Space group	$P2_12_12$	$P4_12_12$	$P4_12_12$
Cell constants *a*, *b*, *c* and *a*, *c* (Å)	57.6, 80.8, 58.9	58.4, 148.1	58.0, 147.4
No. molecules per asymmetric unit/ % solvent/V_M[a]	1/45.4/2.3	1/40.7/2.1	1/39.6/2.1
Wavelength (Å)	1.0096	0.9330	0.9330
No. measurements	185,107	120,202	74,485
No. unique reflections	26,121	15,723	10,438
Resolution range (Å) (outermost shell)	47.6–1.80 (1.90–1.80)[b]	45.8–2.10 (2.21–2.10)	45.6–2.40 (2.53–2.40)
Completeness (%)	99.9 (100.0)	99.7 (98.3)	99.5 (97.6)
R_{merge}[c] (%)	0.042 (0.182)	0.098 (0.613)	0.067 (0.394)
Average intensity $<<I>/\sigma(<I>)>$	31.6 (10.5)	17.0 (3.6)	21.5 (4.6)
B-factor (Wilson) (Å^2)	18.1	29.4	43.2
Average multiplicity	7.1 (7.0)	7.6 (7.6)	7.1 (5.6)
Resolution range used for refinement (Å)	47.6–1.80	45.8–2.10	45.6–2.40
No. reflections used (test set)	25,437 (652)	14,941 (719)	9948 (490)
Crystallographic *R*-factor (R_{free})[d]	0.160 (0.203)	0.187 (0.234)	0.191 (0.246)
Estimated overall co-ordinate errors based on *R*-factor/R_{free} (Å)	0.111/0.111	0.242/0.193	0.562/0.278
No. protein atoms (asymmetric unit)[e]	2103	2156	2093
No. solvent molecules/ions/ligands[e]	195/1 (Ni^{2+})/5 (glycerol)	66/−/−	28/−/−
r.m.s. deviation from target values			
Bond lengths (Å)	0.015	0.011	0.014
Bond angles (°)	1.65	1.33	1.57
Bonded *B*-factors (Å^2) main-chain/side-chain	1.01/2.90	0.72/1.88	0.73/1.80
Average *B*-factors for protein (Å^2)	19.4	34.7	45.0
Average *B*-factors for BLA atoms (Å^2)/ BLA atom occupancy (%)	–	41.5/100	51.9/100

[a] Matthews or V_M parameter.[91]
[b] Values in parentheses refer to the outermost resolution shell if not indicated otherwise.
[c] $R_{merge} = \Sigma_{hkl}\Sigma_i \mid I_i(hkl) - <I(hkl)> \mid / \Sigma_{hkl}\Sigma_i I_i(hkl)$, where $I_i(hkl)$ is the *i*th intensity measurement of reflection *hkl*, including symmetry-related reflections, and <I(hkl)> its average.
[d] *R*-factor $= \Sigma_{hkl} \mid\mid F_{obs} \mid - k \mid F_{calc} \mid\mid / \Sigma_{hkl} \mid F_{obs} \mid$, where F_{obs} and F_{calc} are the observed and calculated structure factor amplitudes; R_{free}, same for a test set of reflections not used during refinement.
[e] Including atoms with alternate occupancy.

Unbound *versus* acylated forms and structural relatives of MecR1-PBD

Comparison of the unbound and the acylated structures reveals a good agreement of the common 246 C^α atoms, which show an rmsd of 0.48 Å (unbound *versus* pencilloyl complex) and 0.50 Å (unbound *versus* oxacilloyl complex) after optimal superposition. The acylated structures display even closer structural similarity to each other (rmsd 0.26 Å), so that the discussion here is centred on the penicilloyl-acylated form, as its structure was obtained to higher resolution. Reported distances between equivalent atoms refer to differences between this and the unbound form if not indicated otherwise. Overall, there is a slight but significant difference between these two structures in the position of the flap-loop Lα3α4 that is maximal at Lys242 C^α and Lys418 C^α (1.3 Å). This is the region of the loop that widens after the short antiparallel segments in extended conformation. A further noteworthy local deviation is found at the tip of the surface loop Lβ5β6 of the USD (1.3 Å at His535 C^α). However, as the structures compared correspond to different space groups, it cannot be ruled out that these differences are due to different crystal packing constraints. Accordingly, although there is potential for mobility within the LSD, however, it cannot account for the substantial rearrangement of MecR1 during signal transduction. Apart from these differences, there are changes in some side-chains near the active site (see below).

The structure of MecR1-PBD shows the same overall fold as the unbound orthologue BlaR-PBD from *B. licheniformis* (Protein Databank (PDB) access code 1nrf)[51] and the paralogue BlaR1-PBD from *S. aureus*, unbound and benzylpenicillin-acylated (PDB 1xa1, 1xa7),[49] as well as in complex with ceftazidime (PDB 1xkz).[50] These structures show goodness-of-fit *Z*-values[58] of 35.3–37.8, rmsd values of 1.3–1.9 Å over 239–243 aligned residues and sequence identities of 40–44 when compared with unbound MecR1-PBD (Figure 4). For a reference, $Z > 2.0$ is usually indicative of structural relatedness and an alignment of MecR1-PBD with itself renders $Z = 48.4$. The third closest structure is *Pseudomonas aeruginosa* OXA-10 (PDB 1e3u, 1fof; $Z = 33.7$; rmsd 1.7 Å over 237 residues; 23% sequence identity),[59,60] a class-D β-lactamase which, in contrast to other β-lactamases like BlaZ or BlaP, can induce oxacillin hydrolysis.[61] As observed with MecR1-PBD, acylation of BlaR1-PBD does not entail significant structural changes. This is in agreement with the results of biophysical experiments performed on BlaR.[62] However, it should be mentioned that

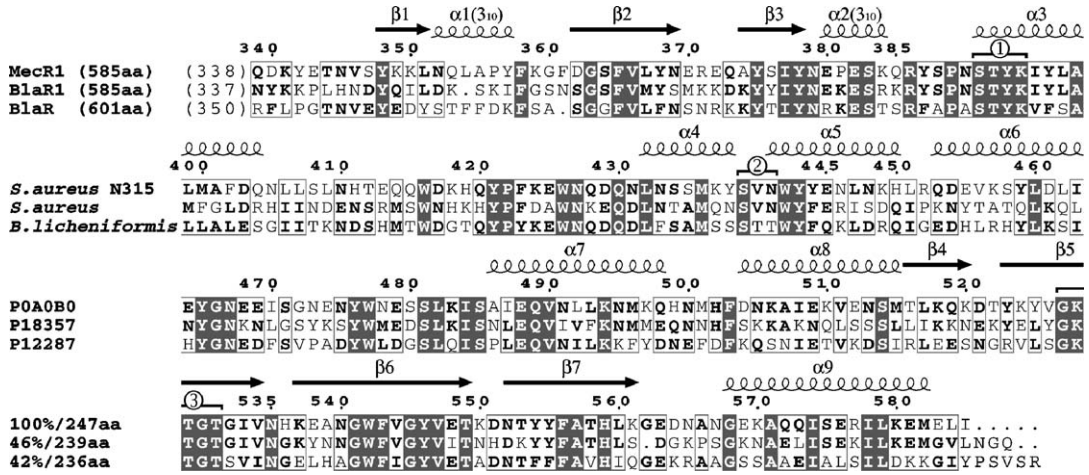

Figure 4. Sequence alignment of structurally characterised extracellular HMW class-C PBD domains of the MecR1/BlaR1 family. The sequences corresponding to the C-terminal domains of pre-MRSA strain N315 MecR1, *S. aureus* BlaR1 and *B. licheniformis* BlaR are shown, together with the number of amino acid residues of each protein and the number of additional N-terminal residues of the full-length protein (first alignment block), the organism and the Swiss-Prot sequence-database access codes (second and third blocks) and the percentage of sequence similarity with MecR1 according to program SIM[90] within the number of overlapping residues (fourth block). Strictly conserved positions are in white over black and positions occupied by similar residues and those conserved in two of the three sequences are in bold and framed. The regular secondary structure elements and their labels, as well as the sequence numbering, correspond to the MecR1-PBD structure. The three characteristic conserved active-site motifs (① to ③) are also marked (see also Figure 3(d)).

these structural relatives of MecR1-PBD are responsible for triggering a resistance response through the synthesis of a penicillinase or β-lactamase (exerted by BlaR and BlaR1) and OXA-10 is itself such a β-lactamase. MecR1, in contrast, triggers biosynthesis of a helper PBP. Contrary to the cognate transcriptional repressors, MecI/BlaI, BlaR1 and MecR1 are not functionally interchangeable and they have distinct kinetics: while *S. aureus* BlaR1 induces BlaZ synthesis within minutes, MecR1 takes hours to switch on production of MecA.[63] This means that, despite gross similarity in the fold, significant differences must be present among MecR1-PBD and its structural relatives to account for these functional differences (see below).

The MecR1-PBD active site

The active site centre of MecR1-PBD is the catalytic serine residue at the beginning of helix α3, Ser391 (Spl391 and Sox391 in the complexes; for atom numbering of the acylated serine residues, see Figure 3(a)). This residue is included in one of the three sequence signatures conserved within PBPs/β-lactamases, the Ser-Xaa-Xaa-Lys motif,[28] which includes Lys394 (① in Figure 4).[28,60] Ser391 is preceded by Asn390, the only residue of the polypeptide that adopts an unfavourable main-chain conformation in all unbound and acylated structures presently reported ($\Phi = 45°$ to $49°$; $\Psi = -128°$ to $-133°$), as it is placed in a generous ε region of a Ramachandran-plot.[64] This main-chain conformation is promoted by Pro389 and enables the active-site serine residue to adopt the position and conformation required for substrate binding. The lower boundary of the active-site cleft is provided by loop Lα3α4, in particular by segments Ser439-Val440-Asn441 within the second consensus sequence, Ser-Xaa-Asn (② in Figure 4), and Pro422-Trp426, further away from the cleft. The top of the cleft is delimited by the USD β-sheet strand β5, which runs horizontally from left to right, creating an upper rim or edge (Figures 2(b) and 3(d) and (e)). This strand includes the conserved Lys528-Thr529-Gly530-Thr531 sequence of the third motif, Lys-Thr/Ser-Gly-Xaa (③ in Figure 4), which binds the stem peptide C terminus and the BLA thiazolidine carboxylate group mimicking such a C terminus. In the acylated MecR1-PBD complexes, this carboxylate is constituted by atoms C-10, O-11 and O-12 attached to C9. The back of the cleft is demarcated by helix α3 and Lα6α7 around Asn475–Ser480. In the unbound structure, some extra electron density was found in the active site below the upper-rim strand and close to, but not linked to, Ser391 and Ser439. In the absence of further experimental evidence, this density was tentatively interpreted as two glycerol molecules (from the cryoprotectant). This finding recalls the unbound BlaR1-PBD (PDB 1xa1)[49] and OXA-10 (PDB 1e3u)[59,65] structures, where a pyrophosphate moiety and a gold cyanide complex, respectively, were found. Comparison with the unbound BlaR-PBD structure (PDB 1nrf),[51] whose pocket is empty, unveils that neither the glycerol molecules nor the pyrophosphate mimic the acylated state. They do not impair the unbound conformation.

BLA binding and proposed mechanism of AEC formation

Despite the number of site-directed mutagenesis, structural and biochemical analyses *in vitro*, there is still controversy regarding some aspects of the mechanisms of action of serine-dependent β-lactamases and PBPs.[66] These include the identification

of several secondary residues important for substrate binding and/or catalysis, which are conserved only within the same class of PBPs/β-lactamases.[27] Merely the role of the catalytic serine residue is unanimously accepted, in analogy to serine proteases.[17,67] It should be remarked that MecR1-PBD and its homologues from the *bla* divergons have a different task than than that of β-lactamases and PBPs, despite close overall structure similarity. PBD proteins are not conceived to bind pentaglycine bridges and stem peptides to carry out transpeptidase reactions or to expeditiously hydrolyse and thus inactivate BLAs. Rather, they are assumed to respond to extracellular BLAs. BlaR-PBD, for instance, has been shown to be one of the most sensitive penicillin-binding proteins described,[12,42] triggering very rapid formation of a stable acylated product for a series of assayed penicillin-type and cephalosporin-type BLAs.[68] Once acylated, PBDs transmit a signal through the membrane to elicit the resistance response encoded by the cognate divergon. This function does not require BLA hydrolysis and BlaR-PBD lacks peptidase and β-lactamase activities.[12,42]

MecR1-PBD binds benzylpenicillin and oxacillin, and establishes the resulting AECs in a nearly equivalent manner (Figures 1(b), and 3(d)–(f)). Besides the covalent link to the catalytic serine O^{γ} atom, hydrophobic and hydrophilic interactions maintain the BLAs strongly anchored to the active-site cleft (see Figure 3(f) and below). The binding modus mimics the way metalloproteases bind peptide substrates; namely, in an extended conformation and antiparallel to the upper-rim strand. However, here this strand runs from left to right (Figure 2(b)), i.e. in the direction opposite to that found in these proteases.[56] As previously mentioned, there is no large overall structural deviation upon BLA binding, apart from the observed slight motion of Lα3α4, which could be due to crystal packing. Locally, however, three side-chains undergo significant rearrangements. First, Glu569, on top of the cleft and provided by the C-terminal helix α9, points toward the active-site cleft in the unbound structure and could play an unfavourable role in BLA binding due to electrostatic repulsion: Glu569 $O^{\varepsilon 2}$ in the unbound structure is merely 2.8 Å away from the position of the thiazolidine ring carboxylate atom O-12 in the acylated structures. Concomitant with BLA binding, rotation of ~120° around both the Glu569 χ_1 and χ_2 angles drives the acidic side-chain out toward the bulk solvent. Second, Ile533 is displaced by the proximal benzyl and methylphenylisoxazolyl moieties of the bound BLAs in a motion affecting Lβ5β6. Third, Asn478, in the back of the active-site cleft and provided by the long loop insertion Lα6α7, is rotated by ~90° around its χ_1 angle. In this manner, it bridges Asn390 with Trp477 through two hydrogen bonds (Asn478 $O^{\delta 1}$-Trp447 $N^{\varepsilon 1}$, 3.1 Å; Asn478 $N^{\delta 2}$-Asn390 $O^{\delta 1}$, 3.4 Å), providing additional stabilisation to the active-site cavity after BLA binding.

Again by analogy with proteases, the mechanism by which MecR1 assembles the AEC *via* serine acylation would proceed as follows. The attack of the catalytic Ser391 onto the β-lactam carbonyl atom C-1 would be triggered by Ser439 O^{γ} or an unprotonated Lys394 N^{η} atom (2.7 Å and 2.5 Å away from Ser391 O^{γ} in the unbound structure, respectively; see below) acting as a general-base. Once the negatively charged tetrahedral transition-state intermediate is formed, it would be stabilised by an oxyanion hole created by Ser391 N and Thr531 N. The tetrahedral intermediate would open the ring after the BLA amide nitrogen atom N-13 abstracts the general-base proton (Figures 1(b) and 3(a)) and give rise to the penicilloyl- or oxacilloyl-AEC. These products are stabilised by six hydrogen bonds and two hydrophobic van der Waals interactions in their MecR1 complex. A double inter-main-chain hydrogen bond of Thr531 N and O is observed with atoms O-2 (2.9 Å) and N-14 (3.1 Å) of the BLA moiety (Figure 3(d)). BLA atom O-16 interacts with Asn441 $N^{\delta 2}$ (2.8 Å) and Ser391 O^{γ}, establishing an ester bond with BLA C-1, is hydrogen-bonded by Ser439 O^{γ} (3.3 Å). Furthermore, the BLA carboxylate oxygen atoms O-11 and O-12 are anchored by Thr529 $O^{\gamma 1}$ (2.5 Å) and Thr531 $O^{\gamma 1}$ (2.7 Å), respectively (Figure 3(d)). Finally, the six-membered aromatic rings (comprising atoms C-18–C-23 in benzylpenicillin and C-23–C-28 in oxacillin; see Figure 3(A)) are engaged in hydrophobic interactions with the side-chains of Ile533 and Phe423. The only noteworthy difference between the benzylpencillin and oxacillin complexes is an interaction of atom O-20 of the isooxazolyl ring of the latter with Ile533 N (3.0 Å).

Either Ser439 or Lys394 could play the role of the catalytic triad general-base histidine in serine proteases and activate the nucleophile Ser391 through proton abstraction (Figures 1(b), and 3(d) and (e)). The role of Ser439 in the stabilisation of the acyl intermediate would suggest that the general base is more likely Lys394 (see above),[27,69,70] which is linked through its N^{η} atom to Asn441 $O^{\delta 1}$ in the complex (3.2 Å). On the other hand, the assumption that Ser439 is the general base is possibly less realistic under biological conditions, due to the very high pK_a value of its hydroxyl group. This hypothesis is based on the close presence of Lys528 N^{η}, imbedded in the Ser-Xaa-Xaa-Lys consensus sequence ① and 2.7 Å away from the Ser439 O^{γ} atom in the complex. The latter lysine, if initially unprotonated, could be the intermediate destination of the catalytic-serine proton, similar to the catalytic triad aspartate residue in serine proteases, and transfer it subsequently to the β-lactam N-13 atom to trigger ring aperture, in both cases *via* Ser439 O^{γ}. The Lys528 N^{η} atom is held in position in the complex through an additional hydrogen bond with Thr529 O (2.8 Å) from consensus sequence motif ③. Further arguments for this disjunction on the general base come from the postulate that in the structurally related OXA β-lactamases this function is carried out by a lysine residue equivalent to Lys394 of MecR1. Activation of the serine nucleo-

phile in these related enzymes involves carboxylation of the lysine N^{η} atom,[70] which is sequestered in a very hydrophobic environment in OXA enzymes. This should lead to a low pK_a value of the lysine ε-amino group and favour carboxylation, which results in large structural displacements and perturbations that distinguish between a classical active, carbamate and an inactive, non-carbamate form.[51] Although in all five PBD structures reported to date the conformations correspond to a classical active form, albeit without a carbamate group, these findings must be viewed with care, as the extra atoms present close or at the active site in the theoretically unbound BlaR1-PBD, MecR1-PBD and OXA-10 molecules (see above) could be responsible for a shift of the equilibrium of lysine *N*-carboxylation, and there are a series of structural, biophysical and biochemical studies that support the hypothesis of a carbamated lysine residue required for catalysis in class-D lactamases.[59,69,71]

The large number of interactions in the acylated MecR1-PBD complexes contrasts with the situation in OXA-10. In the latter, several hydrophilic residues that are engaged in MecR1 in hydrogen bonding of the BLA moiety are replaced with hydrophobic residues, like Asn441 → Val117 (MecR1->OXA-10), Asn478 → Leu155 and Asn390 → Ala66. This entails that once the acylation step has occurred, the AEC is not so stabilised in the β-lactamase. Comparison of MecR1-PBD with OXA-10 shows similar openings of their active sites, so that solvent accessibility is unlikely to be a determinant factor to explain the difference between β-lactamases and PBPs with respect to their behaviour in front of BLAs.[18] In contrast, the greater/lower stability of the AEC could facilitate the final hydrolysis step (3 in Figure 1), and the release of the penicilloic acid in the hydrolytic enzyme. It would explain also why hydrolysis is inefficient/slow in PBDs.[12,42]

A structure-based model hypothesis for MecR1 activation and kinetic considerations

As mentioned, MecR1 features an N-terminal integral-membrane 338 residue MecR1-MP domain and a C-terminal 242 residue MecR1-PBD. Secondary structure predictions for MecR1 and BlaR1, as well as previous topological studies on the homologous BlaR protein,[42] suggest that there is potentially a fourfold TM-helix bundle in the MP domains of these sensor/transducer proteins (Figure 3(g)). Following this hypothesis, the N terminus would be extracellular and close to the beginning of the first helix, TM1. A cytoplasmic loop (L1) would connect TM1 with TM2, and an extracellular loop (L2) would connect helices TM2 and TM3. The intracellular insertion between TM3 and TM4 would be responsible for the actual MP activity. The lack of significant conformational changes of the MecR1-PBD structure upon reaction with BLAs strongly suggests the involvement of further parts of MecR1 in signal transduction, although a hypothetical conformational change of the PBD in solution cannot be ruled out. Accordingly, a homology model for the TM bundle and the two loops of MecR1-MP was constructed to examine the potential steric and topologic restrictions governing the domain arrangement. The model was based on the coordinates of an archaeal transducer complex with a tetrahelical TM bundle, secondary structure predictions and threading calculations. Further restraints came from the helical N-terminal segment of MecR1-PBD in its complex with benzylpenicillin, potentially mimicking the interface between TM4 and MecR1-PBD (Figures 2(c), and 3(g) and (h)). These restraints suggested that the PBD is close to the outer cytoplasmic membrane surface, and thus its active-site cleft is reachable for interaction with loop L2. Moreover, an interaction between L2 and the PBD domain had been observed during phage display experiments with BlaR. This interaction had been shown to be disturbed by acylation with BLAs.[62] In addition, *in vivo* mutation studies on BlaR1 had revealed the importance of two conserved proline residues at the beginning of L2, equivalent to Pro50 and Pro53 in MecR1, since their mutations to alanine abolished expression of the structural gene of the *bla* divergon.[49] These facts account for the importance of L2 in signal transduction.

Taken together, these features enable us to propose a mechanism for the activation of MecR1 (Figure 3(g) and (h)). This mechanism would entail that the MecR1/MecI switch is (auto)proteolytic and thus irreversible.[72] Accordingly, the intervening proteins must be replenished continually until the antibiotic levels are reduced, thus explaining the autogenous regulation. In the basal state, the extracellular loop L2 would interact with a region of MecR1-PBD including the active-site cleft. The L2/MecR1-PBD interaction would ensure that TM3 is fixed and this, in turn, would maintain the MP domain in a latent state. This state entails that the segment of MecR1-MP between the activation cleavage point and TM4 is kept blocking the access of substrates to the MP active-site cleft but inaccessible to autolysis. If suitable BLAs were present in the extracellular space, they could compete with L2 for binding to the PBD domain. As the reaction of the β-lactam ring with the catalytic serine residue is covalent and the product is refractory to hydrolysis, the binding equilibrium would be displaced toward the AEC and the loop would be forced out of its interacting region around the MecR1-PBD active site. This would confer mobility to or even lead to partial unwinding of TM3, which would be capable of a certain motion across the membrane to the cytosol enabling the autolytic cleavage of bond Glu293-Arg294 (on the basis of studies with BlaR1).[47] This cleavage would release an active TM MP comprising the first 293 residues and helices TM1, TM2 and TM3 of full-length MecR1 (see Figure 3(g) and (h)) that would trigger MecI inactivation. In particular, the MecR1-MP activation occurs within a strongly conserved consensus sequence, Baa-Lys-Arg/Glu-✂-Arg-Baa-Xaa-Xaa-Baa (Baa for bulky hydrophobic residues; see Figure 2(b) of García-Castellanos *et*

al.[44]), supporting the hypothesis of the MP domains showing a rather stringent substrate specificity. In contrast, as reported previously,[44] the inactivation cleavage site of MecI and its BlaI relatives is strongly conserved and follows the pattern Baa-Oaa-Oaa-Asn-↓-Phe-Oaa-Glu/Lys-Xaa-Xaa-Xaa-Oaa (Oaa for apolar residues). It is very unlikely that one and the same protease recognises simultaneously such different cleavage patterns. Accordingly, a further player, putatively activated by the MecR1-MP domain and thus containing the activating cleavage pattern, is likely to intervene in the process, being itself in charge of MecI inactivation.

Finally, the studies presented here provide structural evidence for the reported differences in the activation kinetics in the transcription induction of the structural genes in the *bla* and *mec* operons, and thus in the signal transduction pipeline. These differences could be due to the distinct length of the L2 loops, which varies between ~44 and ~51 residues among MecR1, BlaR1 and BlaR according to TM predictions. A second contributing element could be Glu569, whose side-chain could impair BLA binding (see above), explaining the difficulty MecR1 has in sensing BLAs.[73] The position of this glutamate residue is occupied by lysine in BlaR1-PBD and by serine in BlaR-PBD, residues that should rather favour binding of the negatively charged carboxylate group of the thiazolidine ring. Finally, whereas BlaR1 and BlaR hydrolyse arginine-arginine bonds, MecR1 is cut at a glutamate-arginine bond. This may be less favoured and thus provide a third explanation for the difference in the activation kinetics.

Materials and Methods

Cloning, over-expression and purification of MecR1-PBD

S. aureus strain N315 (pre-MRSA) bacterial cells were grown in Luria-Bertani (LB) broth and lysed with lysostaphin (25 μg/ml). The DNA was extracted as described,[74] and used as a template for PCR amplification of the MecR1-PBD coding sequence. Thermostable $Vent_R$ DNA polymerase (New England Biolabs) was used with oligonucleotide 5′-TTTAATACAAGCACCGCATATGTCTGCACATGTTCAAC-3′ as forward primer and oligonucleotide 5′- GATATTTCATACGTTTTAGGATCCATTATATTAACTCCATTTC- 3′ as reverse primer (purchased from Roche Applied Science). The PCR product was a 799 bp fragment containing an open reading frame (ORF) encoding the residues from Ser334 to Ile585 of MecR1 protein (Swiss-Prot sequence database access code **P0A0B0**). The ORF was flanked by restriction sites for NdeI (5′) and BamHI (3′) and was cloned after digestion with these enzymes into a modified pET-28a expression vector (Novagen) using bacteriophage T4 DNA ligase (Roche Applied Science). In this vector, the encoded thrombin-recognition sequence had been substituted by a tobacco etch virus (TEV) protease cleavage site. Restriction analysis and DNA sequencing confirmed that the coding sequence was properly placed after the sequence encoding a His_6 tag and the protease recognition site. The recombinant plasmid was transformed into *E. coli* BL 21 (DE3) (Novagen) cells by heat-shock treatment and plated. A single colony was cultured overnight in LB medium containing 25 μg/ml of kanamycin. For overexpression, 5 ml of this preparation was added to 500 ml of LB, also under the selective pressure of 25 μg/ml of kanamycin, incubated at 37 °C and induced with 0.1 mM isopropyl-β-D-1-thiogalactopyranoside (IPTG) at an absorbance of 0.75 at 600 nm (A_{600}). Cells were further incubated overnight at 17 °C, harvested by centrifugation and frozen.

Pelleted cells were thawed gently at 4 °C and resuspended in 50 ml of buffer A (20 mM Tris–HCl (pH 8.0), 0.5 M NaCl, 20 mM imidazole) containing DNAse I (Roche Applied Science) and an EDTA-free Protease Inhibitor Cocktail Tablet (Roche Applied Science). Cells were disrupted (Constant Systems) at a pressure of 1.35 bar (1 bar = 10^5 Pa) and subjected to centrifugation at 20,000*g* in a Sorvall centrifuge. The supernatant was passed through 0.22 μm pore size filters and loaded onto a 1 ml HiTrap chelating column (Amersham Biosciences), previously loaded with $NiSO_4$ and equilibrated with buffer A. The His_6-tagged protein was eluted using a linear gradient of buffer B (20 mM Tris–HCl (pH 8.0), 0.5 M NaCl, 300 mM imidazole). EDTA and 1,4-dithio-D,L-threitol (DTT) were added to the protein solution eluted from the column at final concentrations of 0.5 mM and 1 mM, respectively. At this point, the sample was digested with TEV protease at a protease:fusion protein molar ratio of 1:100 for 21 h at room temperature. The resulting protein included the three extra residues glycine, histidine and methionine preceding Ser334 of the chemical sequence of the protein. The protein solution was subsequently dialysed against buffer A and loaded again onto the HiTrap column, previously equilibrated with the same buffer. The flow-through fraction from the column was collected, concentrated in an Amicon Ultra-15 centrifugal filter device (Millipore) with a molecular weight cut-off of 10,000 Da and loaded onto a Superdex™ 75 10/300 GL column (Amersham Biosciences) for size-exclusion chromatography using buffer C (20 mM Tris–HCl (pH 8.0), 0.2 M NaCl). The purity of the sample was assessed by SDS-PAGE (16% polyacrylamide, tricine buffer) and mass spectrometry.

Crystallisation of unbound and acylated MecR1-PBD and diffraction data collection

Equivolumetric hanging drops consisting of 1.8 M tribasic ammonium citrate at pH 7.0 and protein solution at 6.8 mg/ml yielded large macroscopically twinned orthorhombic crystals of unbound MecR1-PBD at 20 °C. In contrast, oxacillin-acylated MecR1-PBD crystals were tetragonal and appeared using 2 M tribasic ammonium citrate at pH 6.5 and a protein solution (6.8 mg/ml) that had been incubated with 1 mM oxacillin (Sigma) for 15 min at room temperature. In these crystals, however, the antibiotic was poorly bound, as checked by preliminary X-ray crystallography studies. To remedy this, crystals were subjected to an overnight soak in crystallisation conditions containing also 30 mM oxacillin. In parallel, microseeding techniques were applied to obtain benzylpenicillin-acylated crystals using crystalline nuclei coming from crushed low-occupancy oxacillin crystals and protein that had been incubated overnight at room temperature with 40 mM benzylpenicillin and subsequently dialysed against 1 mM benzylpenicillin. In this case, the precipitating agent was 1.8 M tribasic ammonium citrate at pH 6.5. These crystals were isosymmetric

and isomorphous to the oxacillin-acylated crystals. Crystals were transferred into a crystallisation solution containing 20% (v/v) glycerol for cryo-protection and flash-vitrified in liquid N_2. Complete data sets were collected on CCD detectors at 100K from a monocrystalline fragment of an unbound MecR1-PBD crystal and from acylated single crystals at the European Synchrotron Radiation Facility (ESRF, Grenoble) (see Table 1). All crystals harboured one molecule per asymmetric unit. Diffraction data were processed with XDS,[75] converted to mtz-format with COMBAT within CCP4,[76] and scaled with SCALA.[77] Table 1 provides statistics on data collection and processing.

Structure solutions and refinement

The structure of unbound MecR1 was solved by Patterson-search techniques employing the standalone version of program AMoRe,[78] diffraction data in the 10–4.0 Å resolution range and the co-ordinates of unbound *S. aureus* BlaR1 PBD as a searching model (PDB 1xa1).[49] A unique solution was obtained at 77.9, 71.1, 21.7, (α, β, γ, in Eulerian angles), 0.2503, 0.1701, 0.2837 (x, y, z, as fractional unit-cell coordinates) with a correlation coefficient in structure factor amplitudes (CC_F) of 28.7% and a crystallographic R-factor of 47.8% after rigid-body refinement with FITING (for definitions, see Table 1 and Navaza;[78] second-highest unrelated peak, $CC_F = 19.4\%$, R-factor = 50.6%). This calculation confirmed $P2_12_12$ as the correct orthorhombic space group. Successively, manual model building on a Silicon Graphics Workstation with Turbo-Frodo† alternated with crystallographic refinement (including TLS refinement) using REFMAC5[79] within the CCP4 suite[76] until the final model was obtained (Table 1). This model included protein residues Asp340 to Ile585 (within a single chain A), a tentatively assigned tetrapeptide of sequence Gly1B-His2B-Met3B-Ser4B, one tentative nickel ion (Ni601W), five glycerol molecules (Gol602W–Gol606W) and 195 solvent molecules (Wat607W-Wat801W). All MecR1-PBD protein residues were in unambiguous electron density and in most-favoured/additionally allowed regions of a Ramachandran plot according to PROCHECK,[80] except for Ser380A and Asn390A, which were in generously allowed regions.

The structure of MecR1-PBD in a covalent complex with benzylpenicillin was solved by Patterson search using the refined co-ordinates of the unbound protein and data in the 15–4.5 Å resolution range. A unique solution was obtained at 18.6, 25.5, 188.2, 0.0138, 0.3998, 0.0852 ($CC_F = 57.9\%$, R-factor = 40.2%; next unrelated peak, $CC_F = 34.7\%$, R-factor = 49.8%). This calculation confirmed $P4_12_11$ as the correct space group. Subsequently, manual model building and crystallographic refinement proceeded as mentioned above. The final model comprised all the residues of the construct, in which the three extra residues at the N terminus resulting from the cloning strategy were given the numbering Gly331A, His332A and Met333A. The molecule was observed to be somewhat more flexible than the unbound form, resulting in some regions of the polypeptide in weak electron density, although the chain tracing was unambiguous. All protein residues were placed in most-favoured/additionally allowed regions of a Ramachandran-plot, except for Ser380A, Asn473A and Asn390A in generously allowed regions. The acylated serine was named Spl391A. Furthermore, 66 solvent molecules (Wat701W–Wat766W) were identified.

The structure of the MecR1-PBD complex with oxacillin was solved by Fourier synthesis employing the unbound MecR1-PBD co-ordinates rotated and translated according to the unique solution of the Patterson search calculations performed for the MecR1-PBD/benzylpenicllin complex structure. Model building and refinement proceeded as described above. This structure displayed the greatest flexibility of the three structures analysed, with several regions of the polypeptide, defined from Asp340A to Ile585A, in weak electron density, although none of them affecting the active site. All protein residues were in most-favoured/additionally allowed regions of a Ramachandran-plot, except for Asn390A and Glu583A, in generously allowed regions. The acylated serine residue was termed Sox391A. Besides, 28 solvent molecules (Wat701W–Wat729W) were identified.

Miscellaneous

As there is only one protein molecule in each asymmetric unit, the suffixes for the MecR1-PBD chains have been omitted from the residue numbering for the presentation of the results and the discussion. Figures were prepared with Turbo-Frodo, SETOR,[81] LIGPLOT[82] and MULTALIN/ESPRIPT.[83,84] Prediction of the MecR1 TM helices was performed with TMHMM2.0[85] and SOSUI.[86] The homology model for the segments of MecR1-MP encompassing the TM helices and the loops connecting TM1 and TM2 and TM2 and TM3, respectively, was constructed on the basis of these predictions, the atomic coordinates of the transmembrane four-helix bundle of the *Natronomonas pharaonis* sensory rhodopsin-II transducer complex (PDB 1hls) together with program THREADER v. 3.5[87] and studies performed on *B. licheniformis* BlaR.[42] Structural similarity searches were performed with DALI‡.[58]

Protein Data Bank accession codes

The final co-ordinates of the unbound MecR1-PBD molecule and its complexes with benzylpencillin and oxacillin have been deposited with the Protein Data Bank with accession codes 2iwb, 2iwc and 2iwd, respectively§. During the deposition procedure, some atoms/residues were renamed/renumbered by the pdb (see remarks section of the PDB entries).

Acknowledgements

S. aureus strain N315 (pre-MRSA) was kindly provided by K. Hiramatsu and co-workers at Juntendo University, Japan. We thank M. Espinosa and G. del Solar from the Centro de Investigaciones Biológicas, C.S.I.C., Madrid, for their supervision of bacterial growth and preparation of DNA. The help provided by EMBL and ESRF synchrotron local contacts during data collection is further acknowledged

† http://www.afmb.univ-mrs.fr/-TURBO-

‡ http://www.ebi.ac.uk/dali

§ http://www.ebi.ac.uk/msd

(ESRF, Grenoble). Robin Rycroft is thanked for helpful suggestions to the manuscript. This work was supported by grants BIO2003-00132, GEN2003-20642 and BIO2004-20369-E from the Spanish Ministry for Science and Technology; ON03-7-0 from the "Fundació La Caixa"; EU FP6 Integrated Project LSHC-CT-2003-503297 "CANCERDEGRADOME"; "AVON-Project" 2005X0648 from the Spanish Association Against Cancer; and SGR2005-00280 from the Generalitat de Catalunya. A.M. acknowledges a postgraduate fellowship from "Fundación Carolina", Spanish Ministry of Foreign Affairs, and R.G.-C. of an FPI PhD fellowship from the Spanish Ministry for Science and Technology. G.M.-F. is a "Juan de la Cierva" Postdoctoral Researcher.

References

1. Jevons, M. P., Rolinson, G. N. & Knox, R. (1961). Celbenin-resistant *Staphylococci*. *Brit. Med. J.* **1**, 124–125.
2. Cohen, M. L. (1992). Epidemiology of drug resistance: implications for a post-antimicrobial era. *Science*, **257**, 1050–1055.
3. Schmitz, F.-J. & Jones, M. E. (1997). Antibiotics for treatment of infections caused by MRSA and elimination of MRSA carriage. What are the choices? *Int. J. Antimicrob. Agents*, **9**, 1–19.
4. Fridkin, S. K., Hageman, J. C., Morrison, M., Sanza, L. T., Como-Sabetti, K., Jernigan, J. A. *et al.* (2005). Methicillin-resistant *Staphylococcus aureus* disease in three communities. *N. Engl. J. Med.* **352**, 1436–1444.
5. Petit, J. F., Muñoz, E. & Ghuysen, J. M. (1966). Peptide cross-links in bacterial cell wall peptidoglycans studied with specific endopeptidases from *Streptomyces albus* G. *Biochemistry*, **5**, 2764–2776.
6. Giesbrecht, P., Kersten, T., Maidhof, H. & Wecke, J. (1998). Staphylococcal cell wall: morphogenesis and fatal variations in the presence of penicillin. *Microbiol. Mol. Biol. Rev.* **62**, 1371–1414.
7. Sugai, M. (1997). Peptidoglycan hydrolases of the *Staphylococci*. *J. Infect. Chemother.* **3**, 113–127.
8. Salton, M. R. J. (1994). The bacterial cell envelope: a historical perspective. In *Bacterial Cell Wall* (Ghuysen, J.-M. & Hakenbeck, R., eds), pp. 1–22, Elsevier, Amsterdam.
9. Salton, M. R. J. (1961). Studies of the bacterial cell wall. VIII. Reaction of walls with hydrazine and with fluorodinitrobenzene. *Biochim. Biophys. Acta*, **52**, 329–342.
10. Stapleton, P. D. & Taylor, P. W. (2002). Methicillin resistance in *Staphylococcus aureus*: mechanisms and modulation. *Sci. Prog.* **85**, 57–72.
11. Meroueh, S. O., Bencze, K. Z., Hesek, D., Lee, M., Fisher, J. F., Stemmler, T. L. & Mobashery, S. (2006). Three-dimensional structure of the bacterial cell wall peptidoglycan. *Proc. Natl Acad. Sci. USA*, **103**, 4404–4409.
12. Goffin, C. & Ghuysen, J. M. (2002). Biochemistry and comparative genomics of SxxK superfamily acyltransferases offer a clue to the mycobacterial paradox: presence of penicillin-susceptible target proteins versus lack of efficiency of penicillin as therapeutic agent. *Microbiol. Mol. Biol. Rev.* **66**, 702–738.
13. Schleifer, K. H. & Kandler, O. (1972). Peptidoglycan types of bacterial cell walls and their taxonomic implications. *Bacteriol. Rev.* **36**, 407–477.
14. Biarrotte-Sorin, S., Maillard, A. P., Delettré, J., Sougakoff, W., Arthur, M. & Mayer, C. (2004). Crystal structures of *Weissella viridescens* FemX and its complex with UDP-MurNac-peptapeptide: insights into FemABX family substrates recognition. *Structure*, **12**, 257–267.
15. Kopp, U., Roos, M., Wecke, J. & Labischinski, H. (1996). Staphylococcal peptidoglycan interpeptide bridge biosynthesis: a novel antistaphylococcal target? *Microb. Drug Resist.* **2**, 29–41.
16. Blumberg, P. M. & Strominger, J. L. (1974). Interaction of penicillin with the bacterial cell: penicillin-binding proteins and penicillin-sensitive enzymes. *Bacteriol. Rev.* **38**, 291–335.
17. Waxman, D. J. & Strominger, J. L. (1983). Penicillin-binding proteins and the mechanism of action of β-lactam antibiotics. *Annu. Rev. Biochem.* **52**, 825–869.
18. Ghuysen, J. M. (1991). Serine β-lactamases and penicillin-binding proteins. *Annu. Rev. Microbiol.* **45**, 37–67.
19. Bush, K. & Mobashery, S. (1998). How β-lactamases have driven pharmaceutical drug discovery. From mechanistic knowledge to clinical circumvention. *Advan. Expt. Med. Biol.* **456**, 71–98.
20. Boyle-Vavra, S., Challapalli, M. & Daum, R. S. (2003). Resistance to autolysis in vancomycin-selected *Staphylococcus aureus* isolates precedes vancomycin-intermediate resistance. *Antimicrob. Agents Chemother.* **47**, 2036–2039.
21. Park, J. T. & Strominger, J. L. (1957). Mode of action of penicillin. *Science*, **125**, 99–101.
22. Labischinski, H. (1992). Consequences of the interaction of β-lactam antibiotics with penicillin binding proteins from sensitive and resistant *Staphylococcus aureus* strains. *Med. Microbiol. Immunol.* **181**, 241–265.
23. Liras, P. & Martín, J. F. (2006). Gene clusters for β-lactam antibiotics and control of their expression: why have clusters evolved, and from where did they originate? *Int. Microbiol.* **9**, 9–19.
24. Wise, E. M., Jr & Park, J. T. (1965). Penicillin: its basic site of action as an inhibitor of a peptide cross-linking reaction in cell wall mucopeptide synthesis. *Proc. Natl Acad. Sci. USA*, **54**, 75–81.
25. Tipper, D. J. & Strominger, J. L. (1965). Mechanism of action of penicillins: a proposal based on their structural similarity to acyl-D-alanyl-D-alanine. *Proc. Natl. Acad. Sci. USA*, **54**, 1133–1141.
26. Bode, W. & Huber, R. (1986). Crystal structure of pancreatic serine endopeptidases. In *Molecular and Cellular Basis of Digestion* (Desnuelle, P., Sjoström, H. & Norén, O., eds), pp. 213–234, Elsevier, Amsterdam.
27. Massova, I. & Mobashery, S. (1998). Kinship and diversification of bacterial penicillin-binding proteins and β-lactamases. *Antimicrob. Agents Chemother.* **42**, 1–17.
28. Ghuysen, J. M. (1994). Molecular structures of penicillin-binding proteins and β-lactamases. *Trends Microbiol.* **2**, 372–380.
29. Crisóstomo, M. I., Westh, H., Tomasz, A., Chung, M., Oliveira, D. C. & de Lencastre, H. (2001). The evolution of methicillin resistance in *Staphylococcus aureus*: similarity of genetic backgrounds in historically early methicillin-susceptible and -resistant isolates and contemporary epidemic clones. *Proc. Natl Acad. Sci. USA*, **98**, 9865–9870.
30. Hiramatsu, K., Kondo, H. & Ito, T. (1996). Genetic base

for molecular epidemiology of MRSA. *J. Infect. Chemother.* **2**, 117–129.
31. Lim, D. & Strynadka, N. C. (2002). Structural basis for the β-lactam resistance of PBP2a from methicillin-resistant *Staphylococcus aureus*. *Nature Struct. Biol.* **9**, 870–876.
32. Chambers, H. F. (2003). Solving staphylococcal resistance to β-lactams. *Trends Microbiol.* **11**, 145–148.
33. Hartman, B. J. & Tomasz, A. (1984). Low-affinity penicillin-binding protein associated with β-lactam resistance in *Staphylococcus aureus*. *J. Bacteriol.* **158**, 513–516.
34. Pinho, M. G., de Lencastre, H. & Tomasz, A. (2001). An acquired and a native penicillin-binding protein cooperate in building the cell wall of drug-resistant *Staphylococci*. *Proc. Natl Acad. Sci. USA*, **98**, 10886–10891.
35. Katayama, Y., Ito, T. & Hiramatsu, K. (2000). A new class of genetic element, staphylococcus cassette chromosome mec, encodes methicillin resistance in *Staphylococcus aureus*. *Antimicrob. Agents Chemother.* **44**, 1549–1555.
36. Hiramatsu, K., Cui, L., Kuroda, M. & Ito, T. (2001). The emergence and evolution of methicillin-resistant *Staphylococcus aureus*. *Trends Microbiol.* **9**, 486–493.
37. Hiramatsu, K., Asada, K., Suzuki, E., Okonogi, K. & Yokota, T. (1992). Molecular cloning and nucleotide sequence determination of the regulator region of mecA gene in methicillin-resistant *Staphylococcus aureus* (MRSA). *FEBS Letters*, **298**, 133–136.
38. Hiramatsu, K. (1995). Molecular evolution of MRSA. *Microbiol. Immunol.* **39**, 531–543.
39. Sharma, V. K., Hackbarth, C. J., Dickinson, T. M. & Archer, G. L. (1998). Interaction of native and mutant MecI repressors with sequences that regulate mecA, the gene encoding penicillin binding protein 2a in methicillin-resistant *Staphylococci*. *J. Bacteriol.* **180**, 2160–2166.
40. Clarke, S. R. & Dyke, K. G. (2001). Studies of the operator region of the *Staphylococcus aureus* β-lactamase operon. *J. Antimicrob. Chemother.* **47**, 377–389.
41. Novick, R. P. (1962). Staphylococcal penicillinase and the new pencillins. *Biochem. J.* **83**, 229–235.
42. Hardt, K., Joris, B., Lepage, S., Brasseur, R., Lampen, J. O., Frere, J. M. *et al.* (1997). The penicillin sensory transducer, BlaR, involved in the inducibility of β-lactamase synthesis in *Bacillus licheniformis* is embedded in the plasma membrane via a four-a-helix bundle. *Mol. Microbiol.* **23**, 935–944.
43. García-Castellanos, R., Marrero, A., Mallorquí-Fernández, G., Potempa, J., Coll, M. & Gomis-Rüth, F. X. (2003). Three-dimensional structure of MecI: molecular basis for transcriptional regulation of staphylococcal methicillin resistance. *J. Biol. Chem.* **278**, 39897–39905.
44. García-Castellanos, R., Mallorquí-Fernández, G., Marrero, A., Potempa, J., Coll, M. & Gomis-Rüth, F. X. (2004). On the transcriptional regulation of methicillin resistance: MecI repressor in complex with its operator. *J. Biol. Chem.* **279**, 17888–17896.
45. Hackbarth, C. J. & Chambers, H. F. (1993). blaI and blaR1 regulate β-lactamase and PBP 2a production in methicillin-resistant *Staphylococcus aureus*. *Antimicrob. Agents Chemother.* **37**, 1144–1149.
46. Zhu, Y., Englebert, S., Joris, B., Ghuysen, J. M., Kobayashi, T. & Lampen, J. O. (1992). Structure, function, and fate of the BlaR signal transducer involved in induction of β-lactamase in *Bacillus licheniformis*. *J. Bacteriol.* **174**, 6171–6178.
47. Zhang, H. Z., Hackbarth, C. J., Chansky, K. M. & Chambers, H. F. (2001). A proteolytic transmembrane signaling pathway and resistance to β-lactams in *Staphylococci*. *Science*, **291**, 1962–1965.
48. Mallorquí-Fernandez, G., Marrero, A., García-Piquè, S., García-Castellanos, R. & Gomis-Rüth, F. X. (2004). Staphylococcal methicillin resistance: fine focus on folds and functions. *FEMS Microbiol. Letters*, **235**, 1–8.
49. Wilke, M. S., Hills, T. L., Zhang, H. Z., Chambers, H. F. & Strynadka, N. C. J. (2004). Crystal structures of the apo and penicillin-acylated forms of the BlaR1 β-lactam sensor of *Staphylococcus aureus*. *J. Biol. Chem.* **279**, 47278–47287.
50. Birck, C., Cha, J. Y., Cross, J., Schulze-Briese, C., Meroueh, S. O., Schlegel, H. B. *et al.* (2004). X-ray crystal structure of the acylated β-lactam sensor domain of BlaR1 from *Staphylococcus aureus* and the mechanism of receptor activation for signal transduction. *J. Am. Chem. Soc.* **126**, 13945–13947.
51. Kerff, F., Charlier, P., Colombo, M.-L., Sauvage, E., Brans, A., Frère, J.-M. *et al.* (2003). Crystal structure of the sensor domain of the BlaR penicillin receptor from *Bacillus licheniformis*. *Biochemistry*, **42**, 12835–12843.
52. Glusker, J. P. (1991). Structural aspects of metal liganding to functional groups in proteins. *Advan. Protein Chem.* **42**, 1–76.
53. Harding, M. M. (1999). The geometry of metal-ligand interactions relevant to proteins. *Acta Crystallog. sect. D*, **55**, 1432–1443.
54. Bode, W., Chen, Z., Bartels, K., Kutzbach, C., Schmidt-Kastner, G. & Bartunik, H. (1983). Refined 2 Å X-ray crystal structure of porcine pancreatic kallikrein A, a specific trypsin-like serine proteinase. Crystallization, structure determination, crystallographic refinement, structure and its comparison with bovine trypsin. *J. Mol. Biol.* **164**, 237–282.
55. Matthews, B. W., Jansonius, J. N., Colman, P. M., Schoenborn, B. P. & Dupourque, D. (1972). Three-dimensional structure of thermolysin. *Nature*, **238**, 37–41.
56. Gomis-Rüth, F. X. (2003). Structural aspects of the metzincin clan of metalloendopeptidases. *Mol. Biotech.* **24**, 157–202.
57. Richardson, J. S. (1981). The anatomy and taxonomy of protein structure. *Advan. Protein Chem.* **34**, 167–339.
58. Holm, L. & Sander, C. (1998). Touring protein fold space with Dali/FSSP. *Nucl. Acids Res.* **26**, 316–319.
59. Maveyraud, L., Golemi, D., Kotra, L. P., Tranier, S., Vakulenko, S., Mobashery, S. & Samama, J.-P. (2000). Insights into class D β-lactamases are revealed by the crystal structure of the OXA10 enzyme from Pseudomonas aeruginosa. *Structure*, **8**, 1289–1298.
60. Paetzel, M., Danel, F., de Castro, L., Mosimann, S. C., Page, M. G. & Strynadka, N. C. J. (2000). Crystal structure of the class D β-lactamase OXA-10. *Nature Struct. Biol.* **7**, 918–925.
61. Sanschagrin, F., Couture, F. & Levesque, R. C. (1995). Primary structure of OXA-3 and phylogeny of oxacillin-hydrolyzing class D β-lactamases. *Antimicrob. Agents Chemother.* **39**, 887–893.
62. Hanique, S., Colombo, M.-L., Goormaghtigh, E., Soumillon, P., Frère, J. M. & Joris, B. (2004). Evidence of an intra molecular interaction between the two domains of the BlaR1 penicillin receptor during the signal transduction. *J. Biol. Chem.* **279**, 14264–14272.
63. McKinney, T. K., Sharma, V. K., Craig, W. A. & Archer, G. L. (2001). Transcription of the gene mediating methicillin resistance in *Staphylococcus aureus*

(mecA) is corepressed but not coinduced by cognate mecA and β-lactamase regulators. *J. Bacteriol.* **183**, 6862–6868.
64. Morris, A. L., Mac Arthur, M. W., Hutchinson, E. G. & Thornton, J. M. (1992). Stereochemical quality of protein structure coordinates. *Proteins: Struct. Funct. Genet.* **12**, 345–364.
65. Golemi, D., Maveyraud, L., Vakulenko, S., Tranier, S., Ishiwata, A., Kotra, L. P. *et al.* (2000). The first structural and mechanistic insights for class D β-lactamases: evidence for a novel catalytic process for turnover of β-lactam antibiotics. *J. Am. Chem. Soc.* **122**, 6132–6133.
66. Frere, J. M., Dubus, A., Galleni, M., Matagne, A. & Amicosante, G. (1999). Mechanistic diversity of β-lactamases. *Biochem. Soc. Trans.* **27**, 58–63.
67. Fisher, J. F., Meroueh, S. O. & Mobashery, S. (2005). Bacterial resistance to β-lactam antibiotics: compelling opportunism, compelling opportunity. *Chem. Rev.* **105**, 395–424.
68. Duval, V., Swinnen, M., Lepage, S., Brans, A., Granier, B., Franssen, C. *et al.* (2003). The kinetic properties of the carboxy terminal domain of the *Bacillus licheniformis* 749/I BlaR penicillin-receptor shed a new light on the derepression of β-lactamase synthesis. *Mol. Microbiol.* **48**, 1553–1564.
69. Golemi-Kotra, D., Cha, J. Y., Meroueh, S. O., Vakulenko, S. B. & Mobashery, S. (2003). Resistance to β-lactam antibiotics and its mediation by the sensor domain of the transmembrane BlaR signaling pathway in *Staphylococcus aureus*. *J. Biol. Chem.* **278**, 19419–19425.
70. Fuda, C. C. S., Fisher, J. F. & Mobashery, S. (2005). β-Lactam resistance in *Staphylococcus aureus*: the adaptive resistance of a plastic genome. *Cell. Mol. Life Sci.* **62**, 2617–2633.
71. Golemi, D., Maveyraud, L., Vakulenko, S., Samama, J.-P. & Mobashery, S. (2001). Critical involvement of a carbamylated lysine in catalytic function of class D β-lactamases. *Proc. Natl Acad. Sci. USA*, **98**, 14280–14285.
72. Marie-Claire, C., Roques, B. P. & Beaumont, A. (1998). Intramolecular processing of prothermolysin. *J. Biol. Chem.* **273**, 5697–5701.
73. Berger-Bächi, B. & Rohrer, S. (2002). Factors influencing methicillin resistance in *Staphylococci*. *Arch. Microbiol.* **178**, 165–171.
74. López, P., Espinosa, M., Piechowska, M. & Shugar, D. (1980). Influence of bacteriophage PBS1 and phiW14 deoxyribonucleic acids on homologous deoxyribonucleic acid uptake and transformation in competent Bacillus subtilis. *J. Bacteriol.* **143**, 50–58.
75. Kabsch, W. (1993). Automatic processing of rotation diffraction data from crystals of initially unknown symmetry and cell constants. *J. Appl. Crystallog.* **26**, 795–800.
76. CCP4. (1994). The CCP4 suite: programs for protein crystallography. *Acta Crystallog. sect. D*, **50**, 760–763.
77. Evans, P. (1993). Data reduction. In *Data Collection and Processing—Proceedings of the CCP4 Study Weekend 29-30 January 1993* (Sawyer, L., Isaacs, N. & Bailey, S., eds), pp. 114–122, SERC Daresbury Laboratory, Warrington, UK.
78. Navaza, J. (1994). AMoRe: an automated package for molecular replacement. *Acta Crystallog. sect. A*, **50**, 157–163.
79. Murshudov, G. N., Vagin, A. A. & Dodson, E. J. (1997). Refinement of macromolecular structures by the maximum-likelihood method. *Acta Crystallog. sect. D*, **53**, 240–255.
80. Laskowski, R. A., McArthur, M. W., Moss, D. S. & Thornton, J. M. (1993). PROCHECK: a program to check the stereochemical quality of a protein structure. *J. Appl. Crystallog.* **26**, 283–291.
81. Evans, S. V. (1993). SETOR: hardware lighted three-dimensional solid model representations of macromolecules. *J. Mol. Graph.* **11**, 134–138.
82. Wallace, A. C., Laskowski, R. A. & Thornton, J. M. (1995). LIGPLOT: a program to generate schematic diagrams of protein-ligand interactions. *Protein Eng.* **8**, 127–134.
83. Gouet, P., Robert, X. & Courcelle, E. (2003). ESPript/ENDscript: extracting and rendering sequence and 3D information from atomic structures of proteins. *Nucl. Acids Res.* **31**, 3320–3323.
84. Corpet, F. (1988). Multiple sequence alignment with hierarchical clustering. *Nucl. Acids Res.* **16**, 10881–10890.
85. Krogh, A., Larsson, B., von Heijne, G. & Sonnhammer, E. L. (2001). Predicting transmembrane protein topology with a hidden Markov model: application to complete genomes. *J. Mol. Biol.* **305**, 567–580.
86. Hirokawa, T., Boon-Chieng, S. & Mitaku, S. (1998). SOSUI: classification and secondary structure prediction system for membrane proteins. *Bioinformatics*, **14**, 378–379.
87. Jones, D. T., Taylor, W. R. & Thornton, J. M. (1992). A new approach to protein fold recognition. *Nature*, **358**, 86–89.
88. Walsh, C. (2003). *Antibiotics: Actions, Origins, Resistance.* ASM Press, Washington, DC.
89. Richardson, J. S. (1985). Schematic drawings of protein structures. *Methods Enzymol.* **115**, 359–380.
90. Huang, X. & Miller, W. (1991). A time-efficient, linear-space local similarity algorithm. *Advan. Appl. Math.* **12**, 337–357.
91. Matthews, B. W. (1968). Solvent content of protein crystals. *J. Mol. Biol.* **33**, 491–497.

Edited by I. Wilson

(Received 30 May 2006; received in revised form 15 June 2006; accepted 16 June 2006)
Available online 7 July 2006